Distribution of Coexisting Solid and Fluid Phases Alters the Kinetics of Collapse from Phospholipid Monolayers†

Wenfei Yan and Stephen B. Hall*

Departments of Biochemistry and Molecular Biology, Medicine, and Physiology and Pharmacology, Oregon Health & Science University, Portland, Oregon 97239-3098

Received: December 1, 2005; In Final Form: March 21, 2006

To determine how coexistence of liquid-expanded (LE) and tilted-condensed (TC) phases in phospholipid monolayers affects collapse from the air/water interface, we studied binary films containing dioleoyl phosphatidylcholine−dipalmitoyl phosphatidylcholine (DPPC) mixtures between 10 and 100% DPPC. Previously published results established that this range of compositions represents the LE−TC coexistence region at the equilibrium spreading pressure of 47 mN/m. When held at 49.5 mN/m on a captive bubble, the extent of total collapse fit with the LE area predicted by the phase diagram. The kinetics of collapse, however, when normalized for changes in the LE area, slowed with increasing mole fraction of DPPC. Surface area expressed as stretched exponential functions of time yielded an Avrami exponent that decreased from 1 for the homogeneously LE film to 0.3 for DPPC ≥ 70%. Microscopic studies showed that the largest changes in kinetics occurred when either alterations of the initial composition or the process of collapse induced the films to cross the percolation threshold, so that the LE phase became divided into isolated domains. Our results show that although coexisting solid and fluid phases collapse to extents that are independent, the kinetics of collapse, corrected for differences in LE area, depend on the distribution of the two phases.

Introduction

In addition to phase transitions within an air/water interface,[1−3] two-dimensional monolayers can also undergo a transition to form a three-dimensional bulk phase.[4−8] This transition, commonly known as collapse, is physiologically important. In the lungs, specific cells secrete a mixture of constituents that together act as a surfactant, adsorbing to the air/water interface of the thin liquid layer that lines the alveoli and lowering surface tension.[9] When compressed by the shrinking alveolar surface area during exhalation, films of pulmonary surfactant reach and sustain surface pressures (π) well above the equilibrium spreading pressure (π_e) at which the film and the bulk phase coexist under equilibrium conditions.[10−14] The most fundamental unresolved issue concerning the function of pulmonary surfactant is the mechanism by which the films avoid collapse to achieve and sustain these high π values.

Phase behavior within the monolayer is a major determinant of the kinetics by which films collapse. The very different rates at which the fluid liquid-expanded (LE) and solid tilted-condensed (TC) phases collapse are well-known. The studies here determine the extent to which the presence of the two phases together alters the kinetics of that process. The interface between the two phases, for instance, might provide a favorable site for the heterogeneous nucleation of collapse. The percolation threshold, at which the continuous phase in a two-phases system becomes discontinuous, alters the viscosity of monolayers[15] and might affect growth of the collapsed phase. Binary mixtures of dioleoyl phosphatidylcholine (DOPC) and dipalmitoyl phosphatidylcholine (DPPC) provide a system in which the LE and TC phases coexist over a broad range of compositions for which π_e is invariant.[16] In this region, progressive increases in DPPC cause large changes in the relative area of the two phases but their compositions remain fixed. Our experiments determine if each phase collapses independently, such that, in films with different compositions, the kinetics of collapse are determined only by the relative area of the LE and TC phases.

Materials and Methods

Materials. 1,2-dipalmitoyl-*sn*-glycero-3-phosphocholine (DPPC) and 1,2-dioleoyl-*sn*-glycero-3-phosphocholine (DOPC) were obtained from Avanti Polar Lipids, Inc. (Alabaster, AL) and used without further analysis or purification. The fluorescent probe 1,2-dipalmitoyl-*sn*-phosphoethanolamine-*N*-[Lissamine rhodamine-B sulfonyl] (Rh-DPPE) was purchased from Molecular Probes (Eugene, OR) and used without further purification.

All experiments used a subphase containing 10 mM Hepes pH 7.0, 150 mM NaCl, and 1.5 mM $CaCl_2$ (HSC). All chemicals were purchased from Sigma (St. Louis, MO). Water purified using a multicartridge system (Barnstead, Dubuque, IA) had a resistivity greater than 17 mΩ/cm. Glassware was acid-cleaned.

Methods. *Relaxation Experiments*. Measurements of the relaxation kinetics for entire monolayers at constant π used a captive bubble as a "surface balance".[17,18] The continuous interface of the bubble eliminates confining barriers and provides measurements of area that reflect collapse uncompromised by leakage of the compressed film.[19] charged coupled device cameras monitored the bubble along the vertical axis to ensure an axisymmetric shape and along the horizontal axis to capture images through a frame grabber to a desktop computer, which calculated surface tension, π, and surface area from the measured

† Part of the special issue "Charles M. Knobler Festschrift".

* Address correspondence to Stephen B. Hall, Mail Code NRC-3, OHSU, Portland, OR 97239-3098. Telephone: 503-494-6667. Fax: 503-494-7368. E-mail: sbh@ohsu.edu.

10.1021/jp056989z CCC: $33.50
Published on Web 04/20/2006

height and width according to previously published semiempirical algorithms.[20] Small amounts of the phospholipids in chloroform:methanol (1:1, v:v) were deposited at the surface of a bubble floating below an agarose dome in aqueous solution at ambient temperatures of 22 ± 1 °C.[18] The spreading solvent was removed by exhaustive replacement of the subphase.[18] The films were then compressed by using a computer-controlled syringe pump to apply hydrostatic pressure to the subphase and shrink the bubble to achieve the desired π. The spread films were compressed slowly to 45 mN/m and then at 115% vol/s to 49.5 mN/m, after which simple feedback was used to maintain constant π.

Fluorescence Microscopy. Films containing binary mixtures of DOPC and DPPC in a series of mole fractions were studied microscopically. Monolayers containing 0.5 mol % Rh-DPPE were spread in chloroform on a Langmuir trough with a continuous Teflon ribbon barrier (Labcon, Darlington, UK) to an initial π of <5 mN/m. After 30 min for solvent evaporation, films were compressed at ~3 Å^2/(molecule min) to a π of 42−44 mN/m and then at 150 Å^2/(molecule min) to 49.5 mN/m, after which the area was manipulated using simple feedback to maintain a constant π. A Teflon C-shaped mask inserted vertically through the interface minimized thermal drift of the monolayer while fluorescence micrographs were obtained using a Nikon fluorescence microscope equipped with a silicon-intensified target camera (C2400, Hamamatsu Corp., Hamamatsu City, Japan). Images of monolayers were captured using a frame grabber at 1 image/s during the isobaric compressions. Experiments were performed at the ambient temperature of 22 ± 1 °C and replicated at least three times for each composition.

Curve Fitting. Data were fit to specific expressions by iterative application of the Levenberg−Marquardt algorithm to minimize χ^2 using the program Igor (Wavemetrics, Inc., Lake Oswego, OR).

Results

These studies measured collapse at constant π. If molecular area, $\bar{A}$, is also constant, then according to $\dot{A} = \dot{n}\bar{A}$, the area, A, changes at a rate, $\dot{A}$, that is proportional to the rate $\dot{n}$ at which constituents leave the interface. The experimentally accessible change in area then provides the extent of collapse. To eliminate contributions to the changing area from the leakage around or along confining barriers that commonly confounds experiments at high π on standard Langmuir troughs, experiments used a captive bubble as the surface balance. Rates at which spread films collapsed were measured at 49.5 mN/m, just above the onset of collapse at ~47 mN/m,[16] by following the change in area.

Analysis of how coexistence affected the kinetics of collapse required information on the behavior of each phase individually. For monolayers containing DOPC−DPPC mixtures, films with mole fractions of DPPC (X_{DPPC}) between approximately 0.1 and 1.0 contain coexisting LE and TC phases with those compositions.[16] The kinetics of collapse were therefore first determined for each of the coexisting phases individually, using X_{DPPC} of 0.l and 1.0 to obtain homogeneous films with the appropriate compositions.

Films with $X_{DPPC} = 0.1$ collapsed at rates that decreased as the process proceeded. The subsequent analysis, concerning how the presence of two phases affected the kinetics of collapse, could have used any expression that accurately described the collapse of the LE phase. On the basis of the kinetics of other phase transitions, including the collapse of some fluid films containing phospholipids,[21] measurements of A at different times

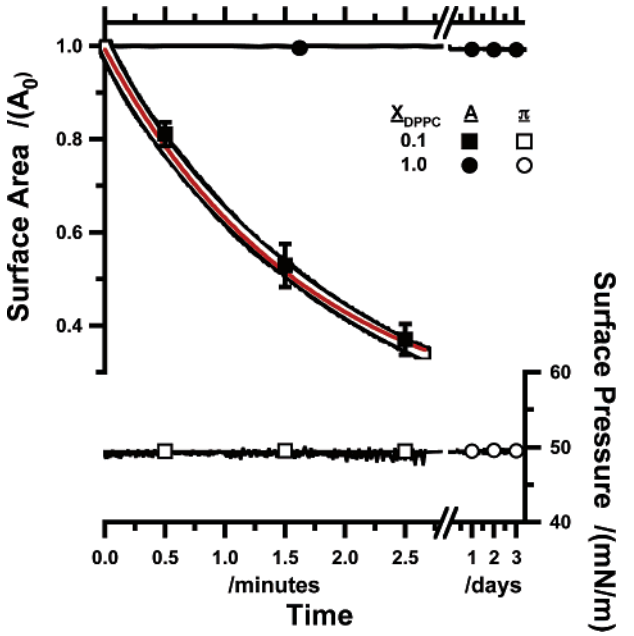

Figure 1. Collapse of films containing the individual phases on captive bubbles. Films containing either $X_{DPPC} = 0.1$ or 1.0 were compressed initially to 45 mN/m and then rapidly to 49.5 mN/m, after which A (left axis) was manipulated to maintain π (right axis) constant. A is normalized to the initial value (A_o) at 49.5 mN/m. Black curves give data for an individual experiment. The symbols ± standard deviation (SD) indicate the variance for at least three experiments, with error bars less than the size of the symbols in some cases, at a few selected points. For measurements of A for $X_{DPPC} = 0.1$, the thick, light gray curve gives the best fit of the data from the individual experiment to eq 2 and the superimposed thin, red curve gives the best fit to that equation with n set to 1. The split time scale indicates the very different behavior of the films with the two compositions.

(t) were fit to the function,

$$A = A_o e^{-(kt)^n} \tag{1}$$

for an initial area A_o. The time constant k and the Avrami exponent n, from the theory of phase transformations,[22−25] were treated as fitting parameters. The data fit the equation well (Figure 1) with values of $n = 0.91 \pm 0.09$ and $k = 0.52 \pm 0.14$ 1/min. The value of n indicated behavior close to that of a simple exponential decay. For n set to 1, which yielded a value of $k = 0.53 \pm 0.13$ 1/min, the fit to the data was comparable (Figure 1). In contrast to the LE films at $X_{DPPC} = 0.1$, for films of pure DPPC, collapse was minimal. The decrease in area required to maintain constant π reached only 0.7 ± 0.2% after 3 days. These results with the individual phases indicated that, for films with coexisting LE and TC phases, an analysis of the kinetics could consider that collapse occurred only from the LE phase.

Films with intermediate compositions collapsed at rates between the two extremes (Figure 2). The kinetics were analyzed in terms of two phases, one with a constant area, $A_1 = A_{1o}$, and a second with area, $A_2(t)$, that decreased as a function of time from an initial area A_{2o} until it collapsed completely. For A_2 expressed according to eq 1,

$$A = A_1 + A_2(t) = A_{1o} + A_{2o}e^{-(kt)^n} = A_\infty + (A_o - A_\infty)e^{-(kt)^n}$$

$$\frac{A}{A_o} = \frac{A_\infty}{A_o} + \left(1 - \frac{A_\infty}{A_o}\right)e^{-(kt)^n} \tag{2}$$

where A_∞ is the final area. If A_∞ was treated as a third fitting

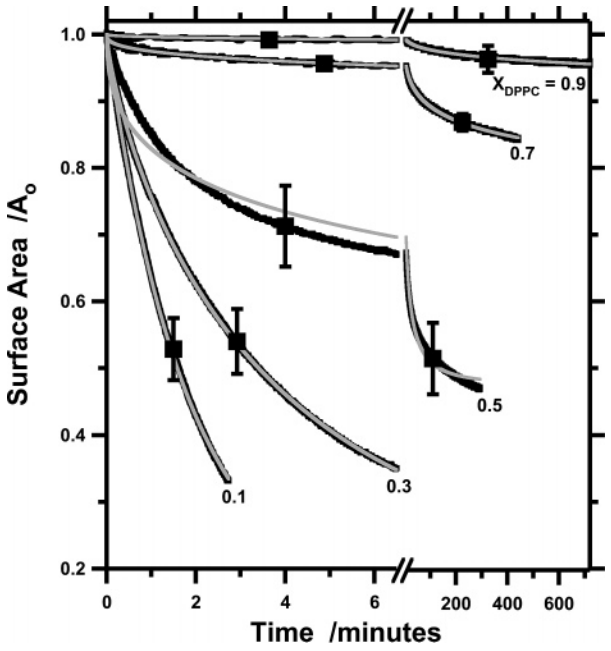

Figure 2. Collapse of films with coexisting phases. Films were compressed rapidly from 45 to 49.5 mN/m and then held at that π. A was normalized to the initial value (A_o) at 49.5 mN/m. Black curves give data from individual experiments, and symbols give the mean ± SD at selected points to indicate the variance of three experiments. Superimposed gray curves give the best fit of the data from the individual experiment to eq 2.

parameter, then data obtained during the collapse of films with different compositions fit eq 2 reasonably well at the higher and lower values of X_{DPPC}, but with significant deviations for intermediate compositions (Figure 2).

If only the LE phase collapsed, then for a film with an area A_c occupied by the TC phase and a total area A_{total}, A_∞/A_o should equal the fractional area A_c/A_{total} occupied by the TC phase prior to the onset of collapse. A_c/A_{total} was obtained from the previously determined phase diagram.[16] For a film with coexisting LE and TC phases, the fraction of the interface occupied by the TC phase, ϕ_c, is given by

$$\phi_c = \frac{A_c}{A} = \frac{\bar{A}_c}{\bar{A}} \frac{(X_{DPPC} - X^e_{DPPC})}{(X^c_{DPPC} - X^e_{DPPC})} \quad (3)$$

where $\bar{A}_c$ and $\bar{A}$ are the molecular areas of the TC phase and the entire film and X^e_{DPPC}, X^c_{DPPC}, and X_{DPPC} are the mole fractions of DPPC for the LE phase, the TC phase, and the entire film, respectively.[26] Values of ϕ_c at π_e were calculated using previously published data.[16] The molecular areas, $\bar{A}$ and $\bar{A}_c$, were obtained from $\pi-A$ isotherms for films with different intermediate compositions and pure DPPC, respectively. The phase diagram indicated values of ~0.08 for X^e_{DPPC} and 1.00 for X^c_{DPPC}. The ratios of A_c/A_{total}, obtained from eq 3, and A_∞/A_o, determined by extrapolation of the individual kinetic curves, agreed well for six compositions from X_{DPPC} values of of 0.1 to 0.9 (Figure 3). In terms of the ultimate extent of collapse at infinite time, the two phases behaved independently.

That independence, however, did not extend to the kinetics of collapse. Equation 2, which accurately described the collapse of films containing only the LE phase, fit the data poorly for X_{DPPC} of 0.4 or 0.5. At X_{DPPC} of 0.7 and 0.9, the value of n was significantly lower than for X_{DPPC} of 0.1, at which the films contained only the LE phase. The compositional dependence suggested that, because collapse of only one phase would alter

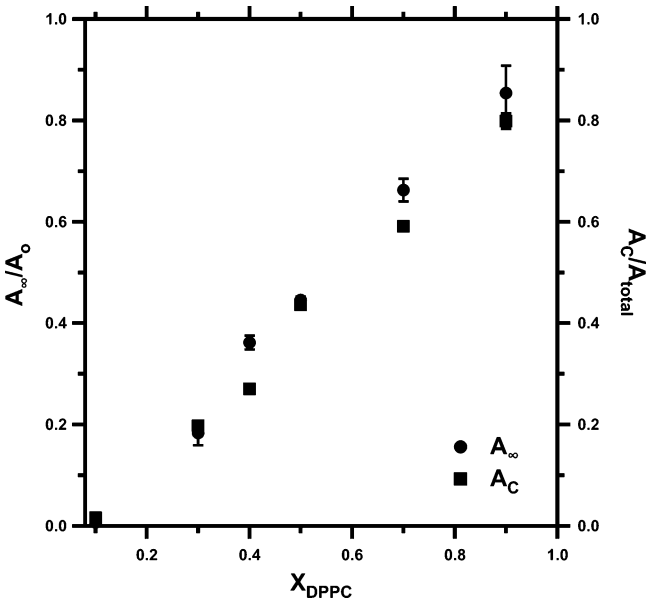

Figure 3. Comparison of TC and extrapolated final areas for films with coexisting phases. A_∞/A_o gives A at infinite time (A_∞), normalized according to the initial area, A_o, at 49.5 mN/m, according to the best fit of eq 2 to the experimental data. A_c/A_{total} indicates the area, A_c, of the TC phase at 47 mN/m, determined from previously published compression isotherms and the fractional areas for the two phases in DOPC−DPPC monolayers.[16] Data are values of the mean ± SD for at least three experiments.

the composition of the remaining film, n might change during the course of an experiment. The variation of n was evaluated[25] by converting eq 2 to the expression

$$\ln\left[-\ln\frac{(A - A_\infty)}{(A_o - A_\infty)}\right] = n(\ln t + \ln k) \quad (4)$$

and constructing plots of

$$\ln\left[-\ln\frac{(A - A_\infty)}{(A_o - A_\infty)}\right]$$

versus ln t, the slopes and intercept of which provided n and ln(k^n), respectively. Values of A_c, obtained from the phase diagram, provided the values of A_∞. These plots tested directly whether the two phases collapsed independently. If n and k depended only on composition, then these variables should be the same for all films in the coexistence region, where only the relative areas of the phases should change, and the plots for the different films should superimpose. The plots also determined if n and k changed when collapse progressed during the course of an experiment.

The shape of these plots varied with the initial composition of the film (Figure 4). At X_{DPPC} of 0.1 and 0.3, the data followed a straight line with constant similar values of n over the entire course of the experiment. For higher compositions, the slope fell during compression so that the final slope, n_f, was significantly less than the initial slope, n_i (Figure 5). For individual experiments with an X_{DPPC} of 0.5, distinct breaks often separated linear segments (Figure 4). The initial segment had slopes similar to those of plots from lower X_{DPPC}, and the final segment was parallel to data from higher X_{DPPC}. Above X_{DPPC} = 0.5, n_f remained constant at approximately 0.3, while n_i fell. Consequently, at X_{DPPC} of 0.7 and 0.9, the differences between n_i and n_f were small and, for most experiments, nonexistent. In all cases, a higher content of DPPC, whether achieved by

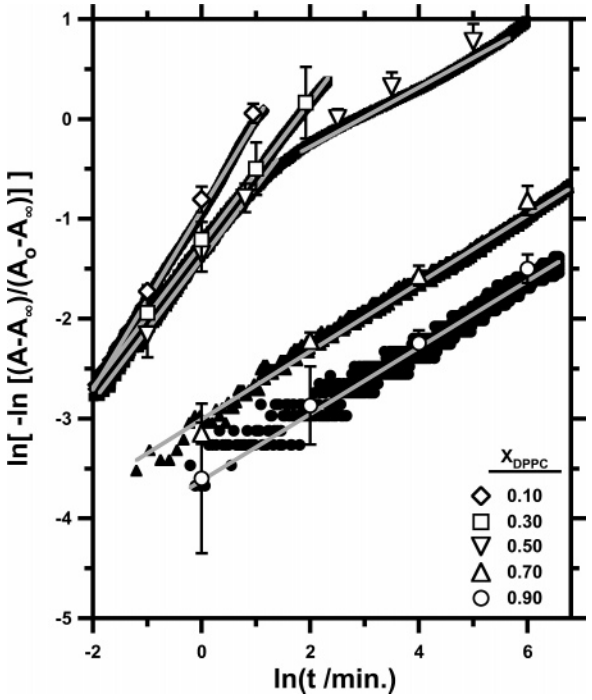

Figure 4. Kinetics of collapse for different compositions, corrected for changes in area of the phase that is capable of collapse. Filled symbols give data points from the individual experiments shown in Figure 2. Open symbols at a few select times indicate the mean ± SD from at least 3 experiments to indicate the variance of the data. Superimposed gray curves are the best fit to eq 4, assuming constant values of n and k for that range of data.

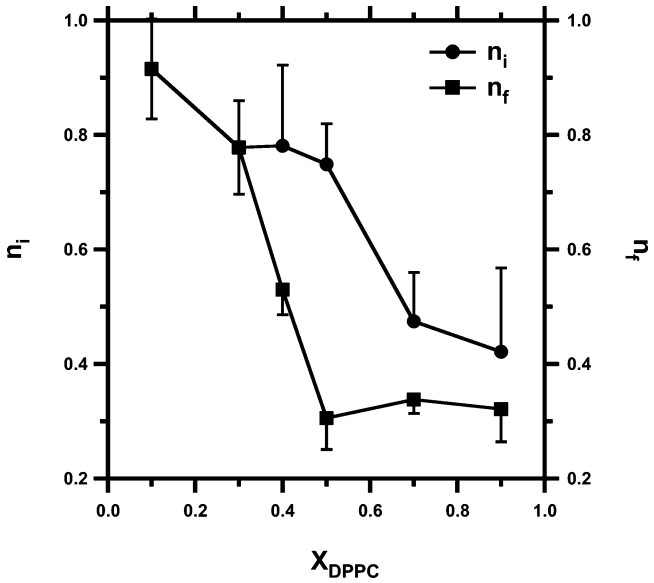

Figure 5. Variation of n with composition. Data from individual experiments were plotted according to Figure 4, and the initial and final slopes were used to obtain values of n_i (left axis) and n_f (right axis), respectively, according to eq 4. Symbols give the mean + SD and the mean − SD for the n_i and n_f values, respectively.

changing the initial composition of the film or by exclusion of the LE phase during collapse, produced smaller values of n, slower collapse, and further deviation from the behavior predicted if the two phases collapsed independently.

Fluorescence microscopy of films on a Langmuir trough showed that in the range of compositions over which n changed most, the distribution of the two phases also changed (Figure 6). Images obtained from films at $X_{DPPC} = 0.4$, 0.5, and 0.7

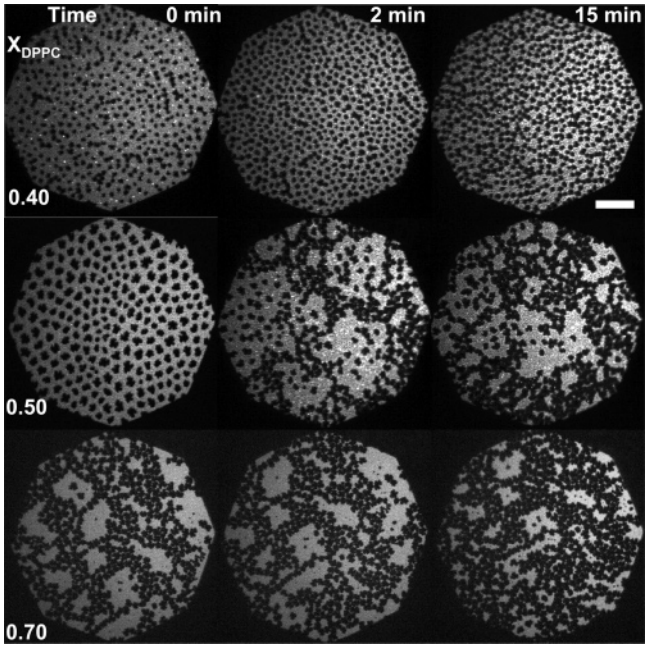

Figure 6. Variation of microscopic appearance with time and composition. Films with different X_{DPPC} and 0.5 mol % Rh-DPPE were spread on a Langmuir trough, compressed at 3 Å^2/(molecule min) to 42−44 mN/m, and then compressed at 150 Å^2/(molecule min) to 49.5 mN/m, after which π was held constant. Micrographs were obtained from monolayers with the indicated compositions at the specified times after completion of the rapid compression. The scale bar indicates a length of 200 μm.

showed phase behavior demonstrated previously for films of DPPC−DOPC compressed to $\pi > \pi_e$ and then allowed to relax at constant area.[16] During continuous compression to 42−44 mN/m, nonfluorescent domains corresponding to the TC phase emerged in fluorescent LE films of all compositions. Intensely fluorescent spots, which previous studies have shown scatter light and represent three-dimensional structures corresponding to collapsed material,[27] appeared during and after the subsequent rapid compression to 49.5 mN/m. The behavior of the nonfluorescent TC domains above π_e, however, was qualitatively different at high and low contents of DPPC. When the nonfluorescent domains first emerged at low π, the TC domains represented the discontinuous phase in all films. For all $X_{DPPC} \leq 0.4$, the domains remained discontinuous during the isobaric compression. At $X_{DPPC} \geq 0.5$, the domains established mutual contact and became the continuous phase, either during or before isobaric collapse, isolating the fluorescent phase into discontinuous islands. In all cases, the higher values of n_i corresponded to initial films that had not reached their percolation threshold and the low values of n_f occurred only with films that had passed beyond that threshold.

The microscopic images of the isolated LE domains provided a second method for monitoring the progression of collapse. The total area of films decreased at faster rates on the trough than on the bubble, suggesting that phenomena at the barriers contributed to the change in area along with collapse of the open film. These phenomena might include creep along or escape around the barriers or collapse nucleated by contact with the barrier. After reaching the percolation threshold, the LE domains provided discrete regions of the film that could be monitored to follow collapse unaffected by the barriers. For a film at $X_{DPPC} = 0.5$, the area of 16 specific domains, and their total area (Figure 6), decreased along a simple exponential function of time (Figure 7). The rate constant k was 0.058 1/min,

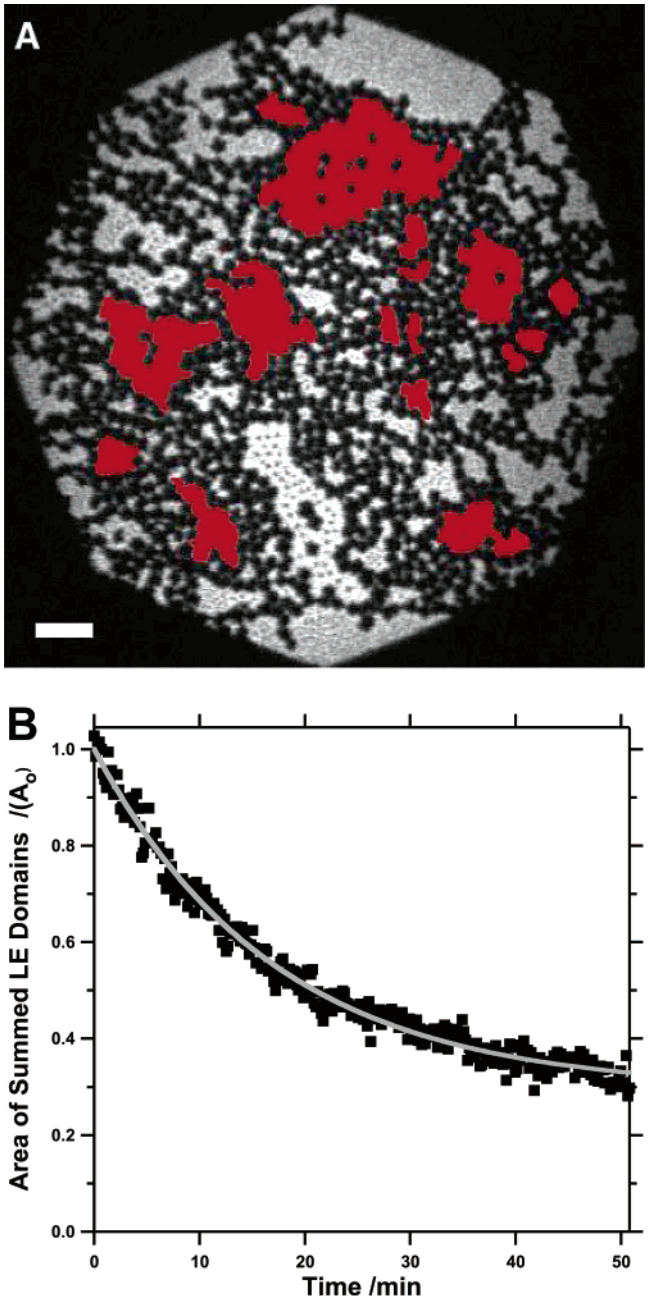

Figure 7. Variation of the area of LE domains with time. A film with an initial X_{DPPC} of 0.5 was spread on a Langmuir trough, compressed slowly to 43 mN/m, and then compressed rapidly to 49.5 mN/m, after which π was held constant. (A) Initial micrograph after reaching the percolation threshold showing 16 LE domains, highlighted in red, each of which remained within the microscopic visual field during 50 min of monitoring at constant π. Only domains with perimeters that never crossed the boundaries of the visual field, so that the area of the complete domain could be measured, were monitored. The scale bar indicates a length of 100 μm. (B) Summed area of the 16 domains at different times. Black squares indicate the experimental data, and the gray curve gives the best fit to the data of the simple exponential $A/A_o = e^{-kt}$, where A_o is the initial area.

lower by an order of magnitude than the value of 0.53 1/min obtained for the homogeneous LE film at $X_{DPPC} = 0.1$ (Figure 1).

Discussion

Our results show that, in films with coexisting solid and fluid phases, although the solid phase has little effect on the extent to which the fluid phase collapses, it can change the kinetics of that process. Within the coexistence region for the LE and TC phases, changes in the binary mixture alter the relative area of the two phases, but not their compositions. The films with intermediate X_{DPPC} ultimately collapse according to the behavior of the individual phases, which show that the LE phase collapses completely and the TC phase not at all. The kinetics of collapse, however, change with composition. With increasing X_{DPPC}, the emergence of the TC domains initially has relatively little effect on the kinetics. The total change in area, $A_o - A_\infty$, varies, but when normalized for that difference, the kinetics of collapse initially change minimally. With higher contents of DPPC, the kinetics slow, at first only late in the process, but with larger X_{DPPC}, during the initial collapse as well. The two phases act independently with respect to the final extent of collapse, but the kinetics depend on their relative areas.

Our microscopic images suggest that the slowing kinetics may reflect changes at the percolation threshold. Films show distinct behavior at X_{DPPC} above and below an intermediate range (Figure 4). The films at low X_{DPPC}, with kinetics that resemble the behavior of the homogeneous LE films, never reach the percolation threshold. At high X_{DPPC}, the films are beyond percolation when they first begin isobaric collapse and the LE phase consists of discontinuous domains from the start. For intermediate compositions, the kinetics change, often at a discrete point or over a narrow interval in time, as collapse progresses. Microscopy shows that, at $X_{DPPC} = 0.5$, the films reach the percolation threshold during compression. At $X_{DPPC} = 0.4$, the films approach percolation during compression that is more limited than that on the captive bubble. Although our inability to monitor kinetics and the microscopic appearance of the same film prevents a firm conclusion, our results suggest that the altered kinetics reflect the changes in the distribution of the LE phase that occur at the percolation threshold.

Collapse of the DOPC−DPPC monolayers occurs on a local basis from individual LE domains. The dimensions of the collapsed structures are much smaller than the LE domains, which shrink as expected while the surrounding solid network is preserved. This process of local collapse is distinct from the large folded bilayers that some films form during collapse and that can have dimensions of milimeters.[8,28−34] The distinction is important for understanding how the percolation threshold affects the kinetics of collapse. The change in viscosity of the entire film that results from a solid network[15] should affect the formation of extended folds. For the local collapse observed here, only changes of the LE domains within the solid network should be important. The slower collapse, therefore, most likely reflects the ability of the solid lattice to partially resist compression so that the individual domains experience a reduced effective surface pressure.

The area of the LE regions decreases along a simple exponential function of time. This observation holds for both the homogeneously LE films and for the isolated LE domains that can be monitored microscopically. The Avrami exponent, n from eq 1, has a value of 1 for these regions that is remarkably low relative to most other phase transitions. When flux from one phase to another can occur anywhere along the interface between them, the rate of the transition increases because growth of the new phase produces a larger interface and the transformation accelerates. Consequently, for standard transitions in three-dimensions[25] and for most transitions considered previously in two-dimensional films,[35,36] n is significantly greater than 1. The bulk phase of hydrated phospholipids, however, is a smectic liquid-crystal, and liquid-crystalline collapse occurs by flow of

the monolayer as a continuous lamella into the new phase,[5,8,27−34,37,38] whether to form the extended bilayer folds or stacks of bilayers adjacent to the monolayer. Movement to the collapsed structure may occur through a region of fixed dimensions.[27] Theoretical analysis shows that the kinetics of such a process should have an n of 1 if nucleation is instantaneous, confined to the very beginning of collapse, or if nucleation occurs at a constant rate but growth stops when the collapsed structures reach a certain size.[21] For mixtures of 30% dihydrocholesterol with DPPC, liquid-crystalline collapse, documented microscopically,[27] proceeds under isobaric conditions along a simple exponential.[21] Because our analysis makes no requirement that we know the mechanism of collapse, we have not proven here that our LE phase exhibits liquid-crystalline collapse. That process, however, seems likely.

When films contain both phases together, area for the entire film decreases along a curve that deviates significantly from a simple exponential. If analyzed in terms of eq 1, the Avrami exponent n decreases further to values well below 1. Prior analysis of the mathematically similar but physically distinct problem of supercooled liquids approaching a glass transition indicates that the deviation of a simple to a stretched exponential behavior can be explained in two ways.[39] The entire system can exhibit the new behavior homogeneously, such that any portion of the system for whatever reason follows the same stretched exponential kinetics. Conversely, the system can become heterogeneous, with different parts all sharing simple exponential decay, but with different time constants, such that

$$A(t) = \sum_i A_{i_o} e^{-\kappa_i t} = \int_0^\infty \rho(\kappa) e^{-\kappa t}\, d\kappa \qquad (5)$$

where $\rho(\kappa)$ gives the distribution of κ values, weighted in terms of areas. Because any monotonic function can be expressed as the Laplace transform of some other function,[40] some form of ρ exists such that

$$A(t) = \int_0^\infty \rho(\kappa) e^{-\kappa t}\, d\kappa = e^{-(\kappa t)^n} \qquad (6)$$

Broader distributions of κ produce lower values of n.

The microscopic images provide some partial support for the heterogeneous explanation. The same simple exponential decrease in area observed for the homogeneous LE film occurs for the individual domains. Isolation of the LE domains within the solid lattice provides a basis for heterogeneous behavior. The rate constant for the LE phase differs by an order of magnitude between the isolated domains and the homogeneous film, demonstrating that the substantial variation in rate constants, which is required to produce the stretched exponential behavior, is possible. The actual rate constants for the domains in our images, however, demonstrate limited heterogeneity. Surveillance of all LE domains within the film might still detect variable rates of collapse, but at this point, the explanation for the very low Avrami constant at high X_{DPPC} remains uncertain.

Concerning the ability of pulmonary surfactant films in situ to avoid collapse, original views discounted kinetic effects such as those demonstrated here. Films were considered only in terms of thermodynamics and the very different rates of collapse for the equilibrium TC and LE phases.[41,42] The prolonged stability of $\pi > \pi_e$ in static lungs is inconsistent with the presence of any fluid phase. Recent observations show, however, that if LE films reach high π, they transform to solid structures that resist collapse.[43−45] Access to high π requires compression faster than the maximum rate of collapse.[46] More graduated effects on the kinetics of collapse, such as the dispersion of coexisting phases, may therefore determine which films with fluid regions can reach the high π where they become metastable.

The phase behavior demonstrated previously in films containing extracts of calf surfactant (calf lung surfactant extract, CLSE) is fluid−fluid rather than the solid−fluid system considered here. With cholesterol present in the biological mixture, the interface between the two coexisting phases can undergo rapid reconfiguration, indicating that both phases must be fluid.[47,48] To the best of our knowledge, the relative kinetics of collapse for these DPPC-rich, or liquid-ordered (l_o), and DPPC-poor, or liquid-disordered (l_d), phases have received little attention. Light scattering microscopy, however, suggests that collapse from a film with these coexisting phases occurs only from the l_d phase.[27] The dispersion of coexisting solid and fluid phases might therefore have the same effects as any fluid−fluid coexistence in biological films.

The temperature dependence of phase behavior complicates the extension of our findings to native pulmonary surfactant. During compression of CLSE films, the l_o phase appears at a π approximately 10 mN/m above the LE−TC transition for DPPC.[47] The l_o−l_d coexistence region for CLSE, with its multiple components, also extends over a much broader range of π than for DPPC.[49] Consequently, at 37 °C, where the main transition for DPPC begins at ∼35 mN/m, the l_o phase in CLSE appears just before the onset of collapse.[49] The dispersion of coexisting phases should, therefore, have little effect on the rates of collapse when that process first begins, although that distribution might become more important if exclusion of the l_d phase would substantially increase the fractional area of the l_o phase. Although the importance of phase separation for native pulmonary surfactant is therefore uncertain, we agree that the dispersion of coexisting phases might affect the behavior of therapeutic surfactants containing simpler mixtures.[15]

Conclusion

In a series of films with solid−fluid coexistence, in which the relative areas of two phases change but not their compositions, the kinetics with which the fluid phase collapses, normalized for its area, depends on the extent of the solid phase. Increasing the solid phase slows collapse, particularly at the percolation threshold where the fluid phase becomes discontinuous. At the threshold, the kinetics change from a simple to a stretched exponential function of time, with the Avrami exponent falling to values of 0.3. Isolated fluid domains continue to show simple exponential kinetics, suggesting that the stretched exponential behavior may reflect heterogeneous time constants in different parts of the film rather than a change to uniformly stretched exponential collapse.

Acknowledgment. The authors thank the following individuals: Drs. Barbora Piknova and Xin-Min Li for initial observations; Drs. Sandra Rugonyi and Alissa Prosser for contributions to the analytical framework; and Chuck Knobler, on this project and many others, for helpful discussions and the inspiration of scientific rigor and clear thinking willingly shared. These studies were supported by the National Institutes of Health (HL60914).

References and Notes

(1) Knobler, C. M. *Science* **1990**, *249*, 870.
(2) Knobler, C. M. *Adv. Chem. Phys.* **1990**, *77*, 397.
(3) Knobler, C. M.; Desai, R. C. *Annu. Rev. Phys. Chem.* **1992**, *43*, 207.
(4) Smith, R. D.; Berg, J. C. *J. Colloid Interface Sci.* **1980**, *74*, 273.

(5) Fang, J. Y.; Knobler, C. M.; Yokoyama, H. *Physica A* **1997**, *244*, 91.
(6) Fang, J. Y.; Dennin, M.; Knobler, C. M.; Godovsky, Y. K.; Makarova, N. N.; Yokoyama, H. *J. Phys. Chem. B* **1997**, *101*, 3147.
(7) Buzin, A. I.; Godovsky, Y. K.; Makarova, N. N.; Fang, J.; Wang, X.; Knobler, C. M. *J. Phys. Chem. B* **1999**, *103*, 11372.
(8) Lu, W. X.; Knobler, C. M.; Bruinsma, R. F.; Twardos, M.; Dennin, M. *Phys. Rev. Lett.* **2002**, *89*, 146107.
(9) Piknova, B.; Schram, V.; Hall, S. B. *Curr. Opin. Struct. Biol.* **2002**, *12*, 487.
(10) Horie, T.; Hildebrandt, J. *J. Appl. Physiol.* **1971**, *31*, 423.
(11) Valberg, P. A.; Brain, J. D. *J. Appl. Physiol.* **1977**, *43*, 730.
(12) Smith, J. C.; Stamenovic, D. *J. Appl. Physiol.* **1986**, *60*, 1341.
(13) Wilson, T. A. *J. Appl. Physiol.* **1981**, *50*, 921.
(14) Schürch, S. *Respir. Physiol.* **1982**, *48*, 339.
(15) Ding, J. Q.; Warriner, H. E.; Zasadzinski, J. A. *Phys. Rev. Lett.* **2002**, *88*, art. no. 168102.
(16) Yan, W.; Piknova, B.; Hall, S. B. *Biophys. J.* **2005**, *89*, 306.
(17) Putz, G.; Goerke, J.; Schürch, S.; Clements, J. A. *J. Appl. Physiol.* **1994**, *76*, 1417.
(18) Crane, J. M.; Putz, G.; Hall, S. B. *Biophys. J.* **1999**, *77*, 3134.
(19) Schürch, S.; Bachofen, H.; Goerke, J.; Possmayer, F. *J. Appl. Physiol.* **1989**, *67*, 2389.
(20) Schoel, W. M.; Schürch, S.; Goerke, J. *Biochim. Biophys. Acta* **1994**, *1200*, 281.
(21) Rugonyi, S.; Smith, E. C.; Hall, S. B. *Langmuir* **2005**, *21*, 7303.
(22) Avrami, M. *J. Chem. Phys.* **1939**, *7*, 1103.
(23) Avrami, M. *J. Chem. Phys.* **1940**, *8*, 212.
(24) Avrami, M. *J. Chem. Phys.* **1941**, *9*, 177.
(25) Christian, J. W. *The Theory of Transformations in Metals and Alloys; an Advanced Textbook in Physical Metallurgy*; Pergamon Press: Oxford, 1965; p 16.
(26) Discher, B. M.; Schief, W. R.; Vogel, V.; Hall, S. B. *Biophys. J.* **1999**, *77*, 2051.
(27) Schief, W. R.; Antia, M.; Discher, B. M.; Hall, S. B.; Vogel, V. *Biophys. J.* **2003**, *84*, 3792.
(28) Ries, H. E., Jr.; Kimball, W. A. Structure of fatty-acid monolayers and a mechanism for collapse. In *Proceedings of the Second International Congress of Surface Activity*; International Union of Pure and Applied Chemistry; Butterworth: London, 1957; Vol. 1 Gas−liquid and liquid−liquid interface, p 75.
(29) Ries, H. E., Jr. *Nature* **1979**, *281*, 287.
(30) Ries, H. E., Jr.; Swift, H. *Langmuir* **1987**, *3*, 853.
(31) Lipp, M. M.; Lee, K. Y. C.; Takamoto, D. Y.; Zasadzinski, J. A.; Waring, A. J. *Phys. Rev. Lett.* **1998**, *81*, 1650.
(32) Gopal, A.; Lee, K. Y. C. *J. Phys. Chem. B* **2001**, *105*, 10348.
(33) Ybert, C.; Lu, W.; Möller, G.; Knobler, C. M. *J. Phys. Chem. B* **2002**, *106*, 2004.
(34) Ybert, C.; Lu, W. X.; Moller, G.; Knobler, C. M. *J. Phys.: Condes. Matter* **2002**, *14*, 4753.
(35) Vollhardt, D.; Retter, U.; Siegel, S. *Thin Solid Films* **1991**, *199*, 189.
(36) Vollhardt, D.; Retter, U. *J. Phys. Chem.* **1991**, *95*, 3723.
(37) de Mul, M. N. G.; Mann, J. A. *Langmuir* **1994**, *10*, 2311.
(38) Friedenberg, M. C.; Fuller, G. G.; Frank, C. W.; Robertson, C. R. *Langmuir* **1994**, *10*, 1251.
(39) Ediger, M. D. *Annu. Rev. Phys. Chem.* **2000**, *51*, 99.
(40) Colmenero, J.; Arbe, A.; Alegria, A.; Monkenbusch, M.; Richter, D. *J. Phys.: Condes. Matter* **1999**, *11*, A363.
(41) Clements, J. A. *Am. Rev. Respir. Dis.* **1977**, *115* (6 part 2), 67.
(42) Bangham, A. D.; Morley, C. J.; Phillips, M. C. *Biochim. Biophys. Acta* **1979**, *573*, 552.
(43) Crane, J. M.; Hall, S. B. *Biophys. J.* **2001**, *80*, 1863.
(44) Smith, E. C.; Crane, J. M.; Laderas, T. G.; Hall, S. B. *Biophys. J.* **2003**, *85*, 3048.
(45) Smith, E. C.; Laderas, T. G.; Crane, J. M.; Hall, S. B. *Langmuir* **2004**, *20*, 4945.
(46) Rugonyi, S.; Smith, E. C.; Hall, S. B. *Langmuir* **2004**, *20*, 10100.
(47) Discher, B. M.; Maloney, K. M.; Grainger, D. W.; Sousa, C. A.; Hall, S. B. *Biochemistry* **1999**, *38*, 374.
(48) Discher, B. M.; Maloney, K. M.; Grainger, D. W.; Hall, S. B. *Biophys. Chem.* **2002**, *101*, 333.
(49) Discher, B. M.; Maloney, K. M.; Schief, W. R., Jr.; Grainger, D. W.; Vogel, V.; Hall, S. B. *Biophys. J.* **1996**, *71*, 2583.